

## **Supplementary Materials for**

## **“The Phylogenetic Hourglass Pattern in Fungi: An Updated Model”**

Yichun Xie et al.

## **Supplementary Text**

Text S1. Materials and Methods.

## **Supplementary Tables**

Table S1. Summary of expression data and reference genomes used in this study.

Table S2. Developmental stages and data source of *Coprinopsis cinerea*.

Table S3. Developmental stages and data source of *Fusarium graminearum*.

Table S4. Developmental stages and data source of *Rhizopus delemar*.

## **Supplementary Figures**

Fig. S1. Life history and developmental processes in the Basidiomycota, *Coprinopsis cinerea*.

Fig. S2. Phylostratigraphic maps.

Fig. S3. TAI split according to the genes from the different phylostrata.

Fig. S4. Heatmaps on relative expression levels in each phylostratum across stages of fungal development.

Fig. S5. Line charts on changes of relative expression levels in each phylostratum across stages of fungal development.

Fig. S6. Mean relative expression levels of old genes (PS1-2) and young genes (PS3-12) across stages of fungal development.

Fig. S7. Number of expressed genes split according to phylostrata.

Fig. S8. Calculation of transcriptome divergence index using reference species from the same Genus (*Rhizopus*) of *R. delemar*.

Fig. S9. Calculation of transcriptome divergence index using reference species from the same Order (Mucorales) of *R. delemar*.

Fig. S10. Calculation of transcriptome divergence index using reference species from the same Phylum (Mucromycota) of *R. delemar*.

Fig. S11. Calculation of transcriptome divergence index using reference species from the same Genus (*Fusarium*) of *F. graminearum*.

Fig. S12. Calculation of transcriptome divergence index using reference species from the same Order (Hypocreales) of *F. graminearum*.

Fig. S13. Calculation of transcriptome divergence index using reference species from the same Class (Sordariomycetes) of *F. graminearum*.

Fig. S14. Calculation of transcriptome divergence index using reference species from the same Phylum (Ascomycota) of *F. graminearum*.

Fig. S15. Calculation of transcriptome divergence index using reference species from the same Family (Psathyrellaceae) of *C. cinerea*.

Fig. S16. Calculation of transcriptome divergence index using reference species from the same Order (Agaricales) of *C. cinerea*.

Fig. S17. Calculation of transcriptome divergence index using reference species from the same Class (Agaricomycetes) of *C. cinerea*.

Fig. S18. Calculation of transcriptome divergence index using reference species from the same Phylum (Basidiomycota) of *C. cinerea*.

Fig. S19. Phylogenetic transcriptomic patterns of all developmental paths in *C. cinerea*.

Fig. S20. Relative expression levels of genes in each phylostratum of *C. cinerea* developmental paths.  
(Fig. S21-32 in Supplementary Material 2).

Fig. S21. KOG annotation on genes split according to phylostrata, fungi.

Fig. S22. KOG annotation on genes split according to phylostrata, animal and plant.

Fig. S23. KOG enrichment analysis on genes following low-high-low or high-low-high expression patterns.

Fig. S24. Dynamics of relative gene expression levels across stages in *R. delemar* development.

Fig. S25. Dynamics of relative gene expression levels across stages in *F. graminearum* development.

Fig. S26. Dynamics of relative gene expression levels across stages in *C. cinerea* development.

Fig. S27. Dynamics of relative gene expression levels across stages in *D. melanogaster* embryogenesis.

Fig. S28. Dynamics of relative gene expression levels across stages in *Da. rerio* embryogenesis.

Fig. S29. Dynamics of relative gene expression levels across stages in *A. thaliana* embryogenesis.

Fig. S30. Dynamics of relative gene expression levels across stages in *A. thaliana* seed germination.

Fig. S31. Dynamics of relative gene expression levels across stages in *A. thaliana* floral transition.

Fig. S32. Cross dissection of pileus under high power microscope (400  $\times$ ).

## Text S1. Materials and Methods

### 1. Data source and transcriptome profiling

Source of transcriptome raw reads and reference genome of all three species were detailed in Table S1-S4 (Kim et al. 2018; Sephton-Clark et al. 2018; Lau et al. 2020; Xie et al. 2020; Xie et al. 2021). Specifically, genomic and transcriptomic data of *C. cinerea* A43mutB43mut pab1-1 #326 was published in our former works. To make it clear, all DNA and RNA samples of *C. cinerea* were collected from the same batch of culture (Fig. S1). RNA libraries were prepared using TruSeq RNA Sample Prep Kit v2 (Illumina, USA) and sequenced with Illumina HiSeq® 4000 at the 2 × 150 bp paired-end read mode. The collection of primordia undergoing meiosis (Pri) and YFB undergoing sporulation were determined by microscopic examination (Fig. S32). Raw reads were aligned to the genome with Hisat2 (Kim et al. 2015). Gene expression levels were calculated and converted into Trimmed Mean of M-values (TMM) using Stringtie (Kovaka et al. 2019) and ‘edgeR’ (Chen et al. 2008) with reference gene model annotations.

### 2. Calculation of phylotranscriptomic indices

Phylostratigraphy was calculated as described in Cheng *et al.* (Cheng et al. 2015) by searching against the NCBI nr database (accessed on March 2, 2022). The ‘diamond blastp’ (Buchfink et al. 2021) was applied to accelerate the search, with ‘--eval 1e-3 -k0’, and default sensitivity option (finding hits of >60% identity and short read alignment). Genes were assigned to the broadest taxonomic level where an ortholog was hit. PS1 (old) to PS10/12 (young) were responding from cellular organisms to species. dN/dS ratio was calculated using ‘dNdS()’ in R package ‘orthologr’ (Drost et al. 2015) with ‘dnds\_est.method = "YN"' (Cheng et al. 2015). Species with complete genome sequences and annotation were selected as the reference species. To minimise the bias, three or more reference species of different phylogenetic distance were obtained. Transcriptome age index (TAI) and transcriptome divergence index (TDI) were calculated with specific functions in R package ‘myTAI’ (Drost et al. 2015). Genes were functionally annotated using eggNOG-mapper v2.1.7 (Cantalapiedra et al. 2021) with eggNOG 5.0 database (Huerta-Cepas et al. 2018). Functional enrichment analyses were performed using ‘compareCluster()’ in R package ‘clusterprofiler’ v4.2.2 (Wu et al. 2021). Statistics and visualisation were performed in R v4.1.2 (R Core Team 2022).

### 3. Data availability

Supplementary files, expression matrix, PS values, dNdS ratio, reference sequences, codes on bioinformatic analyses are distributed at <https://github.com/xieyichun50/Fungal-hourglass>.

## References

- Buchfink B, Reuter K, Drost HG. 2021. Sensitive protein alignments at tree-of-life scale using DIAMOND. *Nat. Methods* 18:366–368.
- Cantalapiedra CP, Hernández-Plaza A, Letunic I, Bork P, Huerta-Cepas J. 2021. eggNOG-mapper v2: Functional Annotation, Orthology Assignments, and Domain Prediction at the Metagenomic Scale. *Mol. Biol. Evol.* 38:5825–5829.
- Chen Y, McCarthy D, Ritchie M, Robinson M, Smyth G. 2008. EdgeR: differential analysis of sequence read count data. :1–119.
- Cheng X, Hui JHL, Lee YY, Law PTW, Kwan HS. 2015. A “developmental hourglass” in fungi. *Mol. Biol. Evol.* 32:1556–1566.
- Drost H-G, Gabel A, Grosse I, Quint M. 2015. Evidence for active maintenance of phylotranscriptomic hourglass patterns in animal and plant embryogenesis. *Mol. Biol. Evol.* 32:1221–1231.
- Huerta-Cepas J, Szklarczyk D, Heller D, Hernández-Plaza A, Forslund SK, Cook H, Mende DR, Letunic I, Rattei T, Jensen LJ, et al. 2018. eggNOG 5.0: a hierarchical, functionally and phylogenetically annotated orthology resource based on 5090 organisms and 2502 viruses. *Nucleic Acids Res.* 47:309–314.
- Kim D, Langmead B, Salzberg SL. 2015. HISAT: a fast spliced aligner with low memory requirements. *Nat. Methods* 12:357–360.
- Kim W, Miguel-Rojas C, Wang J, Townsend JP, Trail F. 2018. Developmental dynamics of long noncoding RNA expression during sexual fruiting body formation in *Fusarium graminearum*. Di Pietro A, editor. *MBio* 9.
- Kovaka S, Zimin A V., Pertea GM, Razaghi R, Salzberg SL, Pertea M. 2019. Transcriptome assembly from long-read RNA-seq alignments with StringTie2. *Genome Biol.* 20:278.
- Lau AYT, Xie Y, Cheung MK, Cheung PCK, Kwan HS. 2020. Genome-wide mRNA and miRNA analysis in the early stages of germ tube outgrowth in *Coprinopsis cinerea*. *Fungal Genet. Biol.* 142:103416.
- R Core Team. 2022. R: a language and environment for statistical computing.
- Sephton-Clark PCS, Muñoz JF, Ballou ER, Cuomo CA, Voelz K. 2018. Pathways of pathogenicity: Transcriptional stages of germination in the fatal fungal pathogen

*Rhizopus delemar*. mSphere 3.

Wu T, Hu E, Xu S, Chen M, Guo P, Dai Z, Feng T, Zhou L, Tang W, Zhan L, et al. 2021. clusterProfiler 4.0: A universal enrichment tool for interpreting omics data. *Innov.* 2:100141.

Xie Y, Chang J, Kwan HS. 2020. Carbon metabolism and transcriptome in developmental paths differentiation of a homokaryotic *Coprinopsis cinerea* strain. *Fungal Genet. Biol.* 143:103432.

Xie Y, Zhong Y, Chang J, Kwan HS. 2021. Chromosome-level *de novo* assembly of *Coprinopsis cinerea* A43mut B43mut pab1-1 #326 and genetic variant identification of mutants using Nanopore MinION sequencing. *Fungal Genet. Biol.* 146:103485.

Table S1. Summary of expression data and reference genomes used in this study.

Species	Reference genome	Developmental stage	BioProject ID	Reference
<i>Coprinopsis cinerea</i>	Genbank GCA_016772295.1	Basidiospore germination	PRJNA560226	(Lau et al. 2020)
<i>A43mut</i> <i>B43mut pab1-1</i> #326	(Xie et al. 2021)	Sexual reproduction	PRJNA573620	(Xie et al. 2020)
<i>Fusarium graminearum</i> PH-1	RefSeq GCF_000240135.3	Spore germination and sexual reproduction	PRJNA429630	(Kim et al. 2018)
<i>Rhizopus delemar</i> RA 99-880	Genebank GCA_000149305.1	Spore germination	PRJNA13066	(Sephton-Clark et al. 2018)

Table S2. Developmental stages and data source of *Coprinopsis cinerea*.

<b>Label</b>	<b>Stage</b>	<b>Incubation</b>	<b>NCBI Run</b>
<b>Spore</b>	Fresh basidiospores	Basidiospore discharged from mature cap	SRR9967573 SRR9967574 SRR9967575
<b>Ger</b>	Half germinating basidiospores	Continuous darkness at 37 °C for 12 h, broth 150 rpm	SRR9967570 SRR9967571 SRR9967572
<b>Brch</b>	Fully germinated basidiospores and branching hyphae	Continuous darkness at 37 °C for 24 h, broth 150 rpm	SRR9967567 SRR9967568 SRR9967569
<b>Myc</b>	Vegetative mycelia	Continuous darkness at 37 °C for 4 d	SRR10162454 SRR10162463 SRR10162464
<b>Knot</b>	Mycelia with hyphal knots	Continuous darkness at 37 °C for 5.5 d, and 12 h:12 h light–dark cycle for 1 d	SRR10162448 SRR10162449 SRR10162450
<b>Pri</b>	Primordia undergoing meiosis	Continuous darkness at 37 °C for 5.5 d, and 12 h:12 h light–dark cycle for 6 d	SRR10162447 SRR10162461 SRR10162462
<b>YFB</b>	Young fruiting bodies undergoing spore formation	Continuous darkness at 37 °C for 5.5 d, and 12 h:12 h light–dark cycle for 6.5 d	SRR10162458 SRR10162459 SRR10162460
<b>Oidia</b>	Oidia forming mycelia	Continuous light at 37 °C for 4 d	SRR10162451 SRR10162452 SRR10162453
<b>Scl</b>	Sclerotia forming mycelia	Continuous darkness at 37 °C for 12 d	SRR10162455 SRR10162456 SRR10162457

Table S3. Developmental stages and data source of *Fusarium graminearum*.

<b>Label</b>	<b>Stage</b>	<b>Description</b>	<b>NCBI Run</b>
(As listed in Kim et al. 2018)			
<b>Spore</b>	G0	Fresh asexual spore macroconidia	SRR6464121 SRR6464122 SRR6464123
<b>Polar</b>	G1	Germination of macroconidia at polar growth stage	SRR6464124 SRR6464125 SRR6464126
<b>Elong</b>	G2	Germination of macroconidia at doubling of long axis stage	SRR6464127 SRR6464128 SRR6464129
<b>Brch</b>	G3	Germinated macroconidia and branching of hyphae	SRR6464130 SRR6464131 SRR6464132
<b>Myc</b>	S0	Vegetative stage	SRR6464097 SRR6464098 SRR6464099
<b>PIni</b>	S1	Formation of perithecial initial	SRR6464100 SRR6464101 SRR6464102
<b>PWall</b>	S2	Formation of perithecial walls	SRR6464103 SRR6464104 SRR6464105
<b>Para</b>	S3	Formation of paraphyses (sterile cells supporting perithecia)	SRR6464106 SRR6464107 SRR6464108
<b>Asci</b>	S4	Formation of asci (saclike structures in which ascospores develop)	SRR6464109 SRR6464110 SRR6464111
<b>MP</b>	S5	Formation of ascospores (meiospores) in mature perithecia	SRR6464112 SRR6464113 SRR6464114

Table S4. Developmental stages and data source of *Rhizopus delemar*.

<b>Label</b>	<b>Stage</b>	<b>Description</b>	<b>NCBI Run</b>
(As listed in Sephton-Clark et al. 2018)			
<b>Spore</b>	0 h	Dormant	SRR7167797 SRR7167798 SRR7167799
<b>Swell1</b>	1 h	Swelling	SRR7167796 SRR7167802 SRR7167803
<b>Swell2</b>	2 h	Swelling	SRR7167795 SRR7167800 SRR7167801
<b>Polar</b>	3 h	Swelling	SRR7167794 SRR7167806 SRR7167807
<b>Elong1</b>	4 h	Swelling, germ tube emergence	SRR7167808 SRR7167809 SRR7167811
<b>Elong2</b>	5 h	Germ tube emergence	SRR7167810 SRR7167812 SRR7167813
<b>Brch</b>	6 h	Germ tube emergence, hyphal growth	SRR7167790 SRR7167804 SRR7167805
<b>Hy1</b>	12 h	Hyphal growth	SRR7167791 SRR7167792 SRR7167793
<b>Hy2</b>	16 h	Hyphal growth	SRR7167786 SRR7167787 SRR7167788
<b>Hy3</b>	24 h	Hyphal growth	SRR7167784 SRR7167785 SRR7167789

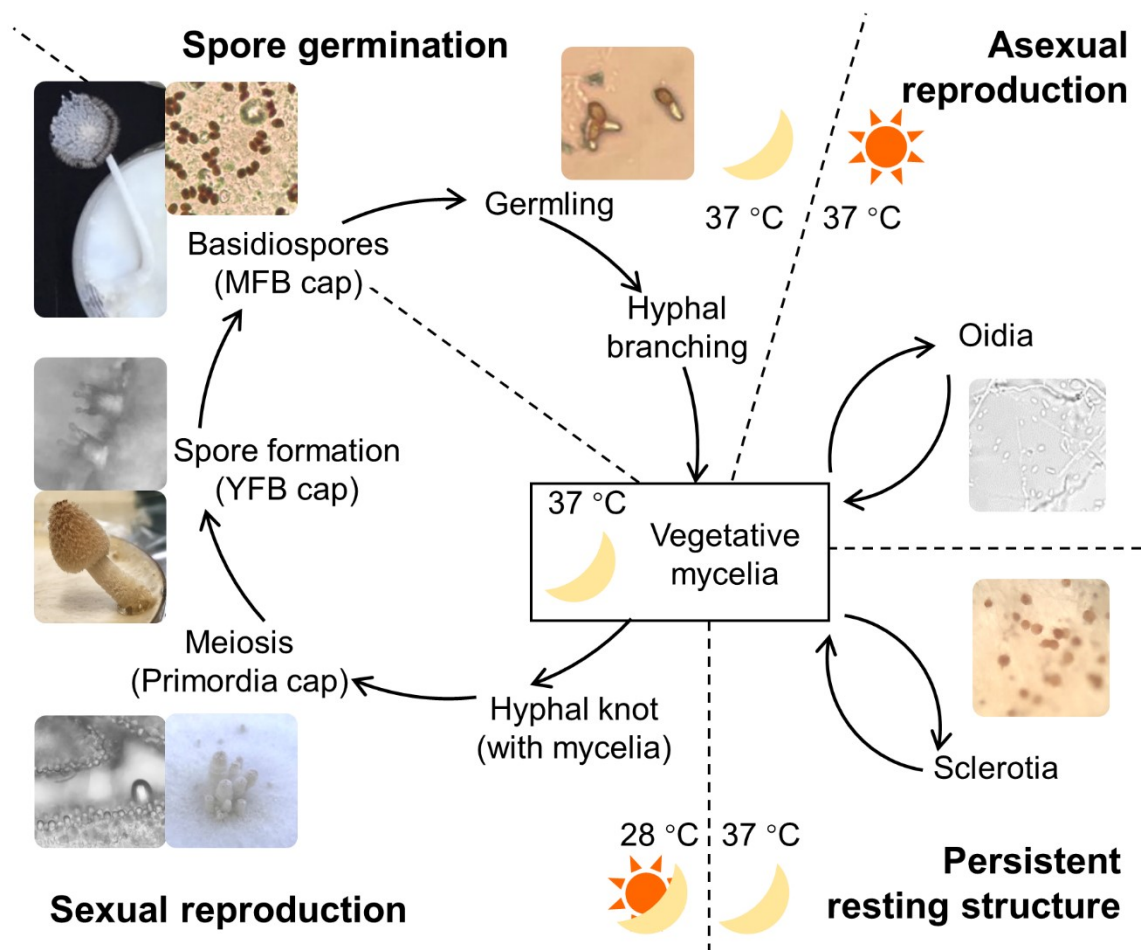
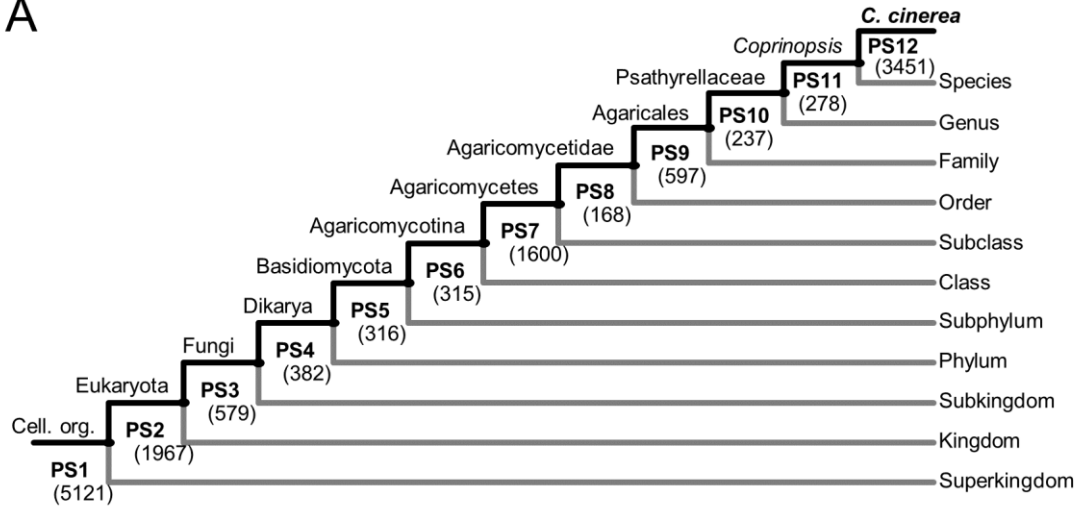
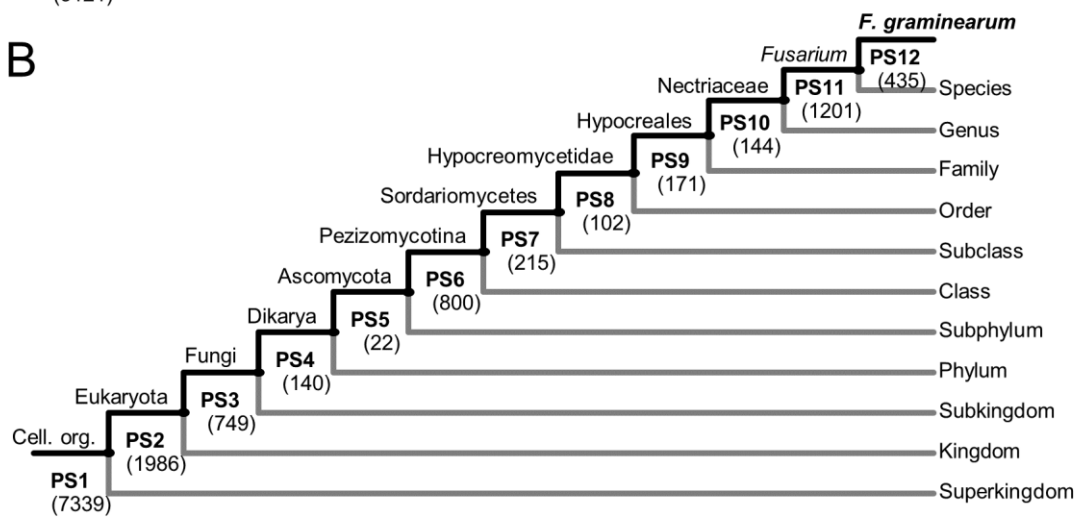


Fig. S1. Life history and developmental processes in the Basidiomycota, *Coprinopsis cinerea*.

A



B



C

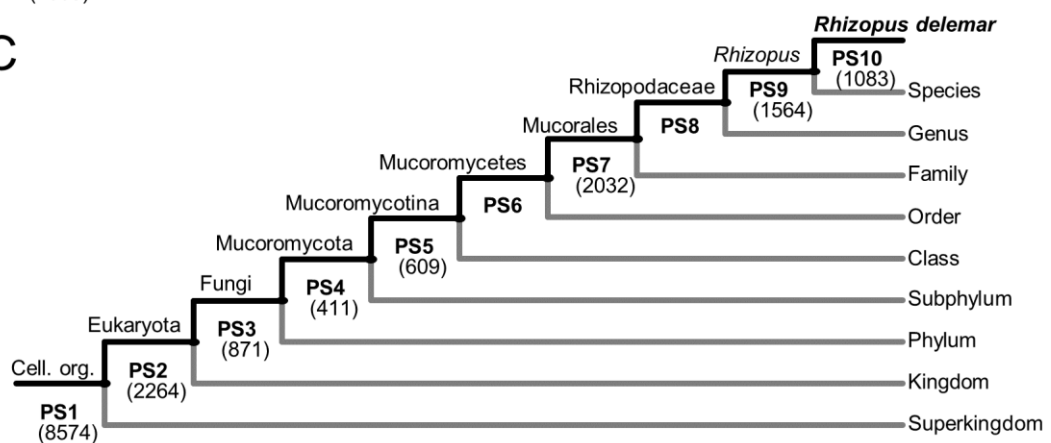


Fig. S2. Phylostratigraphic maps. (A) *C. cinerea*; (B) *F. graminearum*; (C) *R. delemar*.

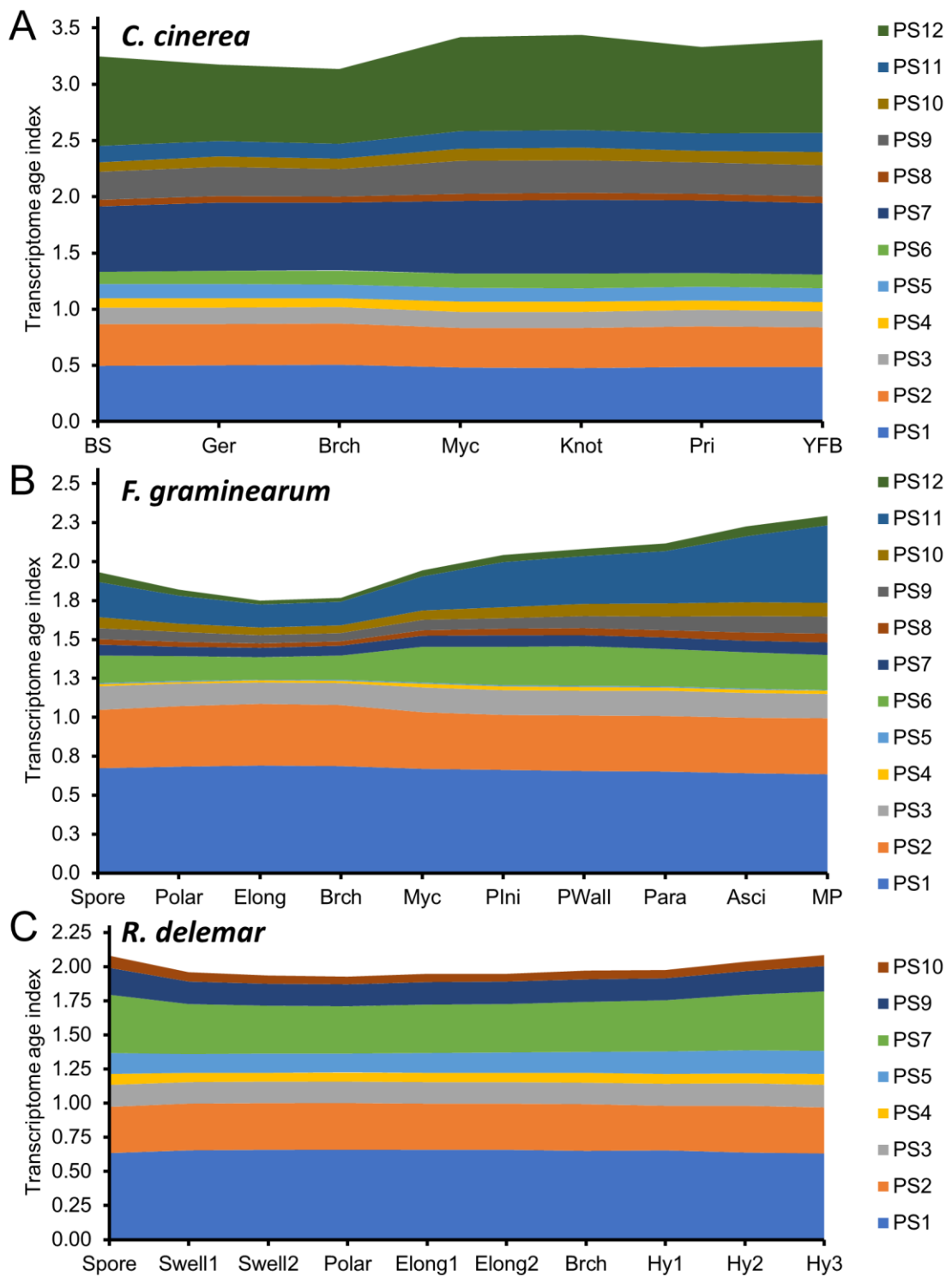


Fig. S3. TAI split according to the genes from the different phylostrata. (A) *C. cinerea*; (B) *F. graminearum*; (C) *R. delemar*.

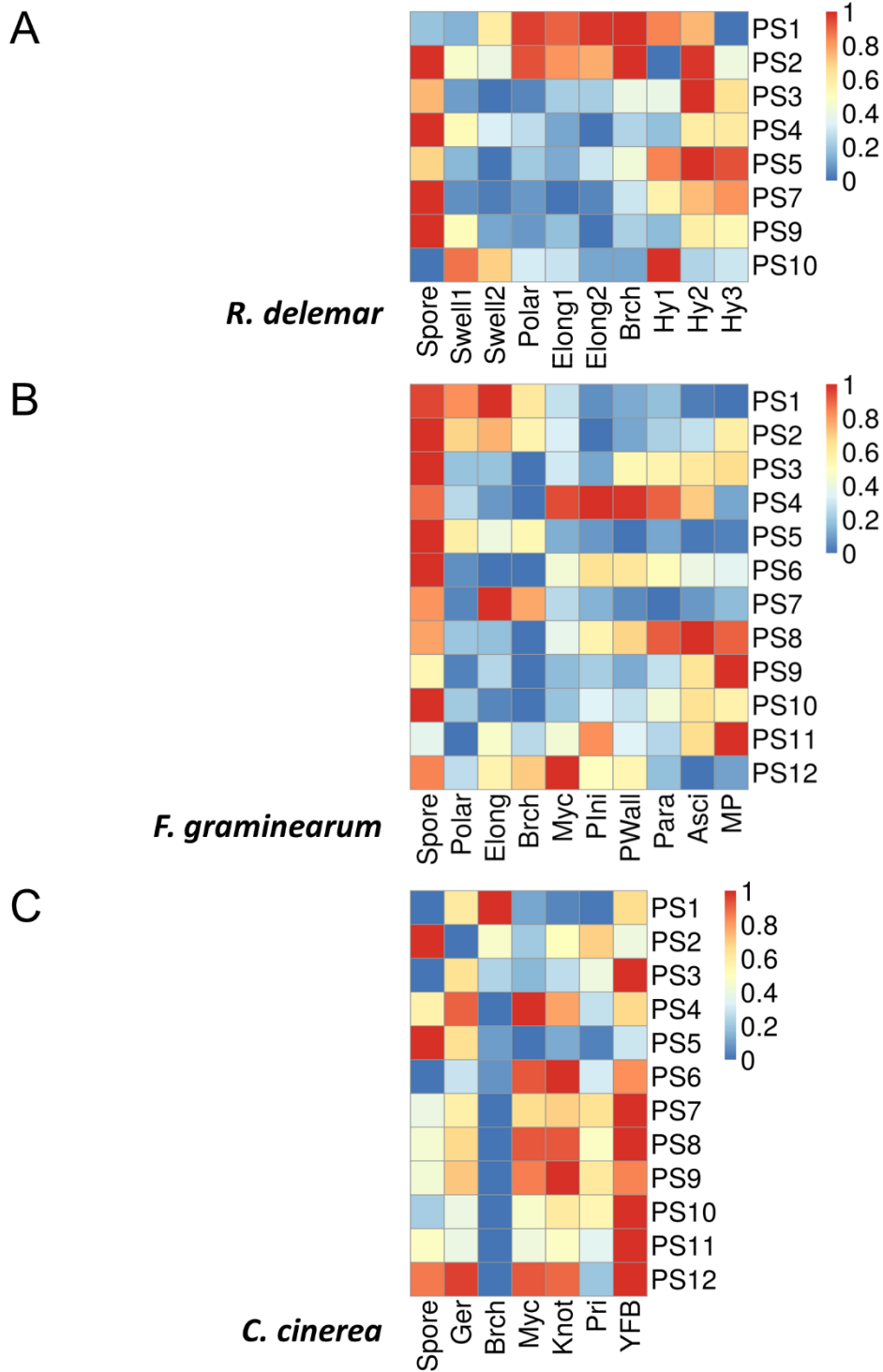


Fig. S4. Heatmaps on relative expression levels in each phylostratum across stages of fungal development. (A) *R. delemar*; (B) *F. graminearum*; (C) *C. cinerea*.

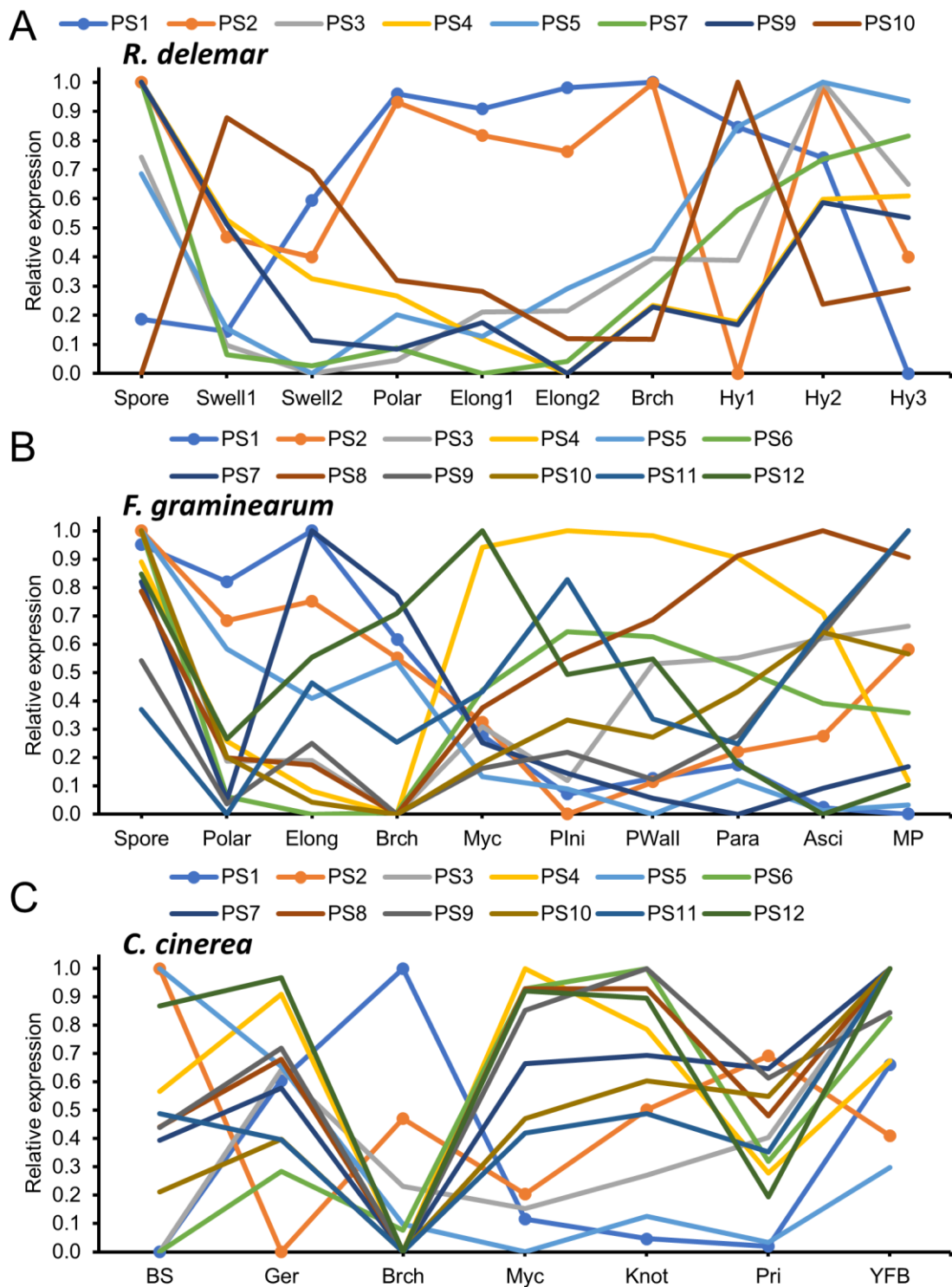


Fig. S5. Line charts on changes of relative expression levels in each phylostratum across stages of fungal development. (A) *R. delemar*; (B) *F. graminearum*; (C) *C. cinerea*.

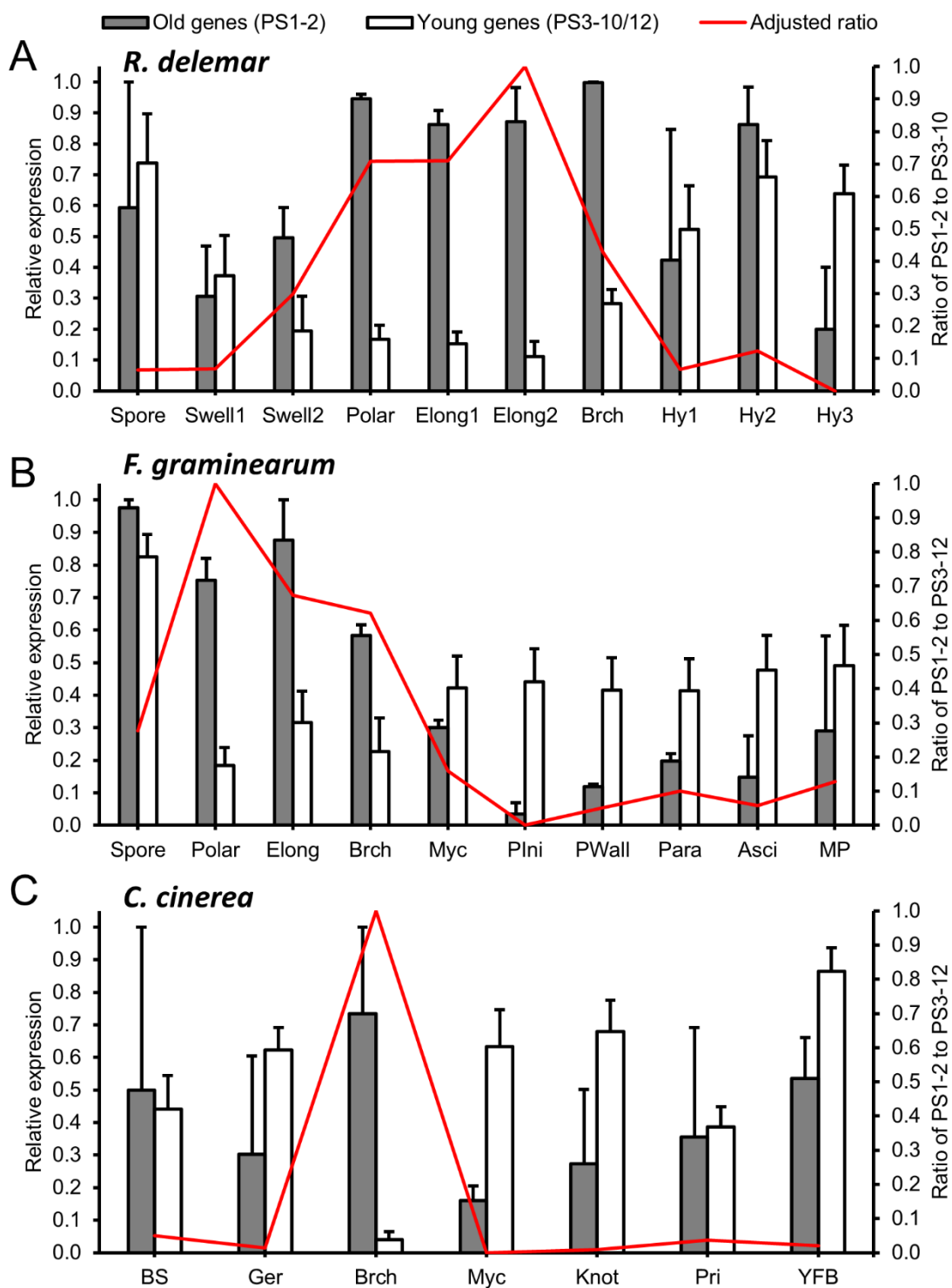


Fig. S6. Mean relative expression levels of old genes (PS1-2) and young genes (PS3-12) across stages of fungal development. Left axis is scaled for relative expression levels that showed in bars and error bars indicated standard errors. Right axis is scaled for adjusted ratio of mean relative expression levels between old genes and young genes. (A) *R. delemar*; (B) *F. graminearum*; (C) *C. cinerea*.

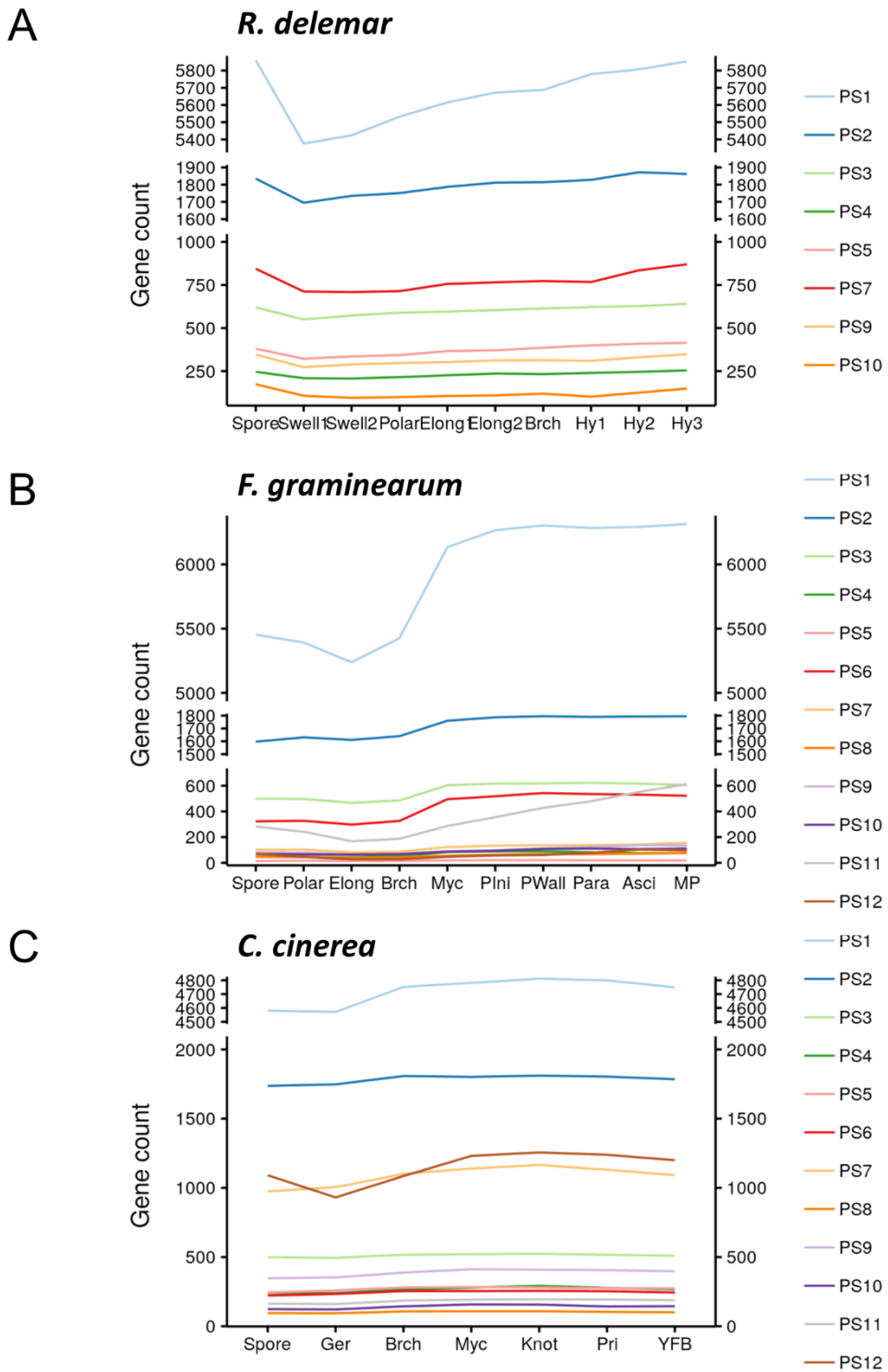


Fig. S7. Number of expressed genes split according to phylostrata. (A) *R. delemar*; (B) *F. graminearum*; (C) *C. cinerea*.

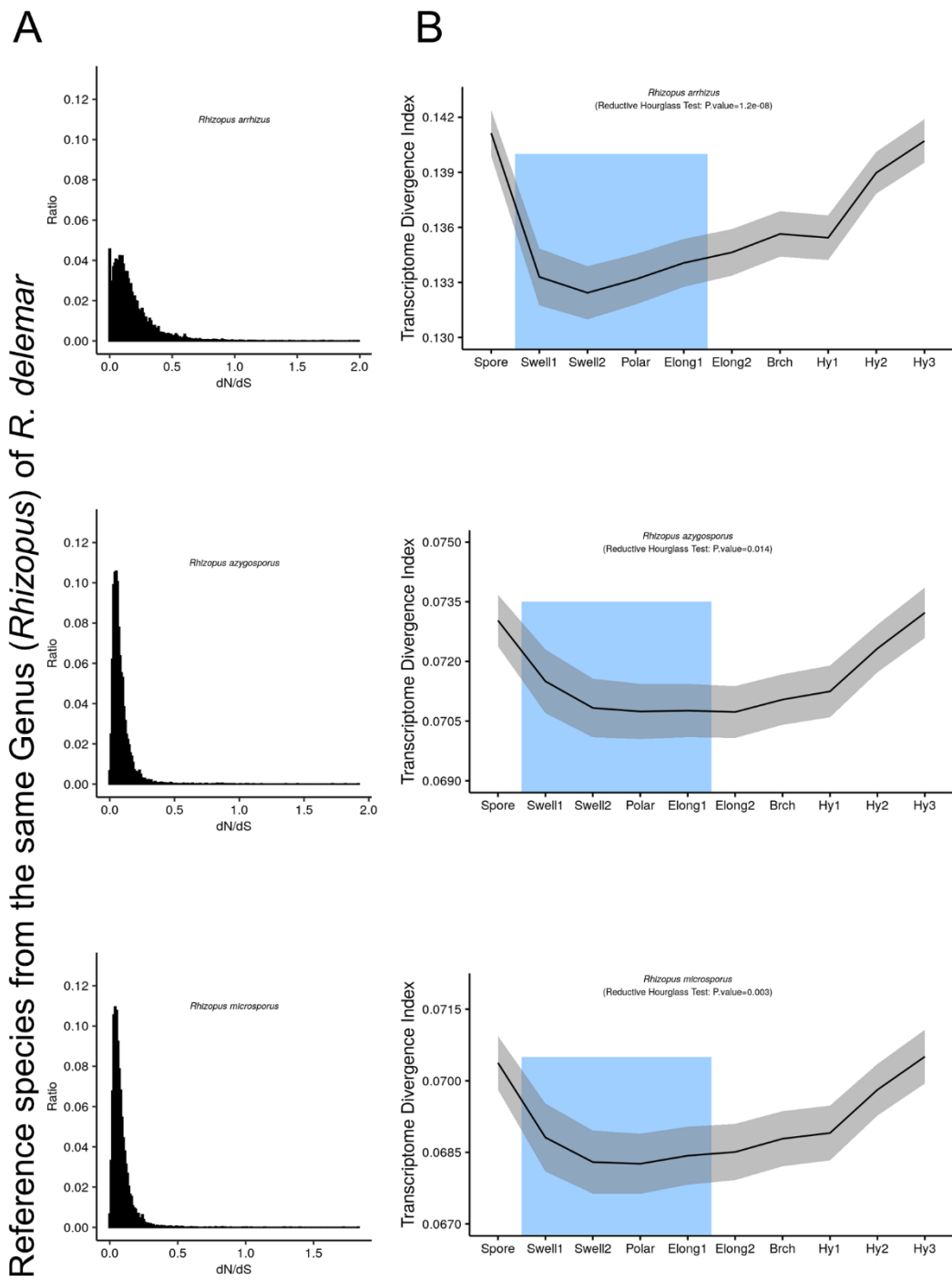


Fig. S8. Calculation of transcriptome divergence index using reference species from the same Genus (*Rhizopus*) of *R. delemar*. (A) Distribution of dN/dS ratio; (B) TDI profile, p values are derived by application of the reductive hourglass test.

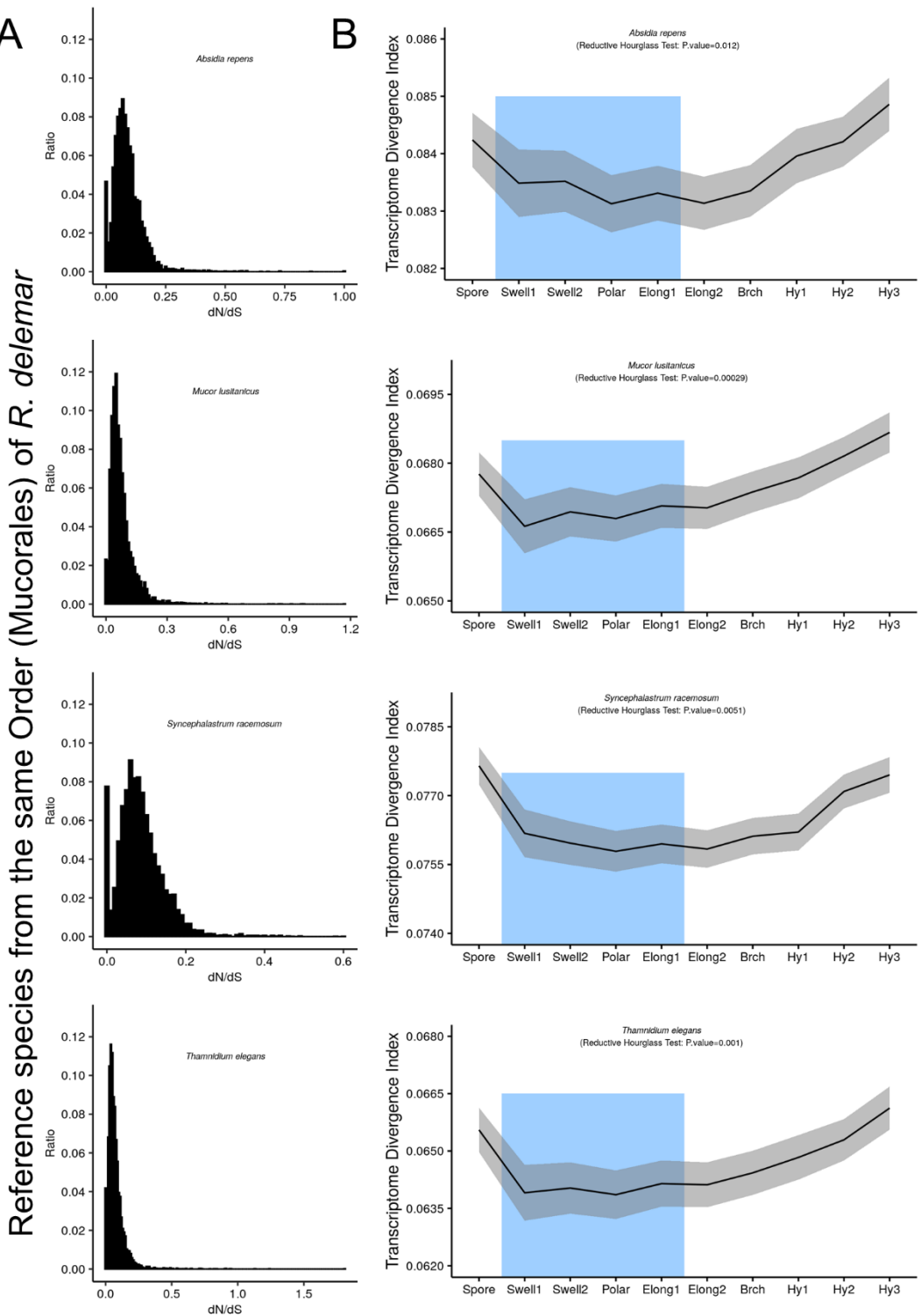


Fig. S9. Calculation of transcriptome divergence index using reference species from the same Order (Mucorales) of *R. delemar*. (A) Distribution of dN/dS ratio; (B) TDI profile, p values are derived by application of the reductive hourglass test.

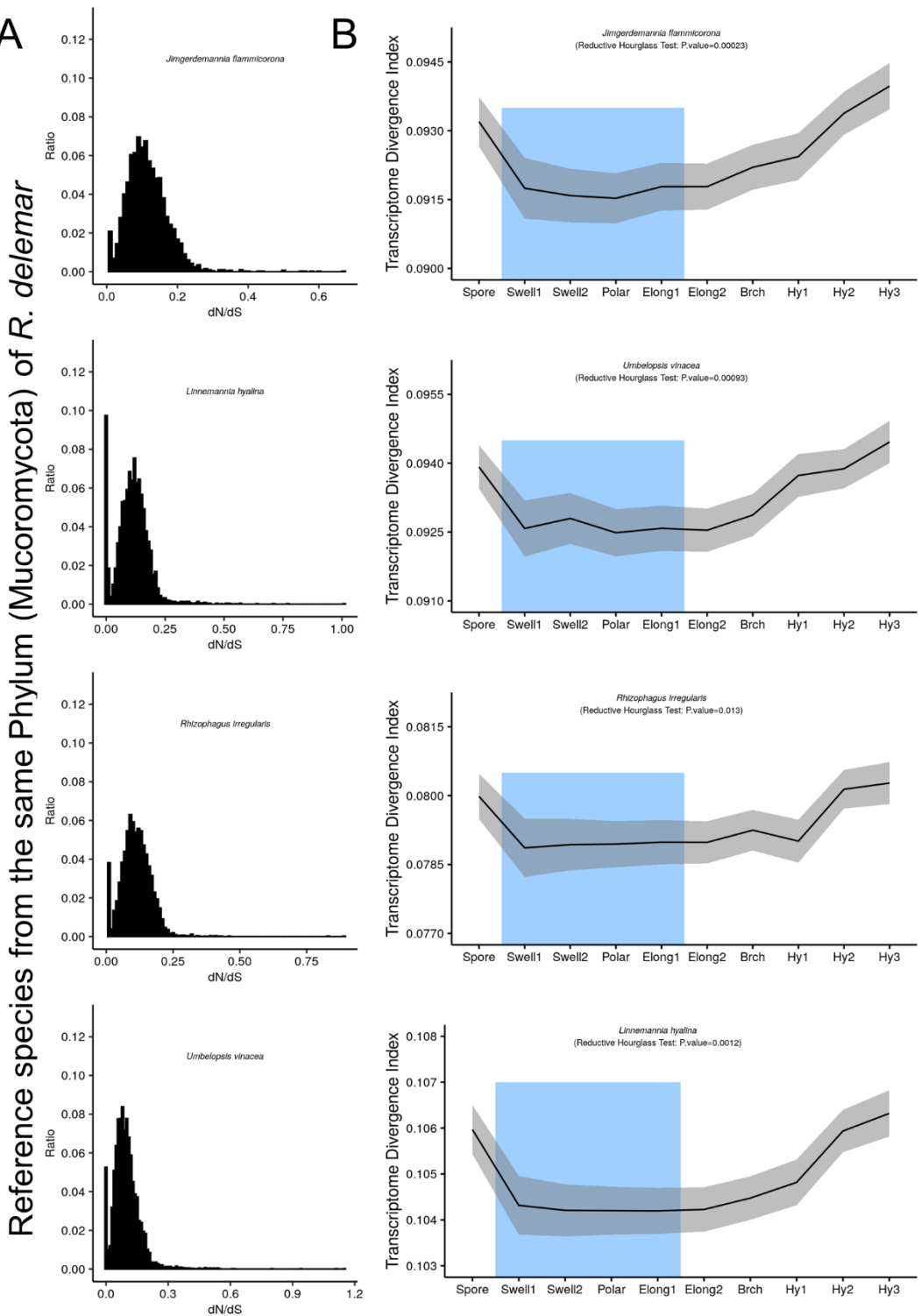


Fig. S10. Calculation of transcriptome divergence index using reference species from the same Phylum (Mucoromycota) of *R. delema*. (A) Distribution of dN/dS ratio; (B) TDI profile, p values are derived by application of the reductive hourglass test.

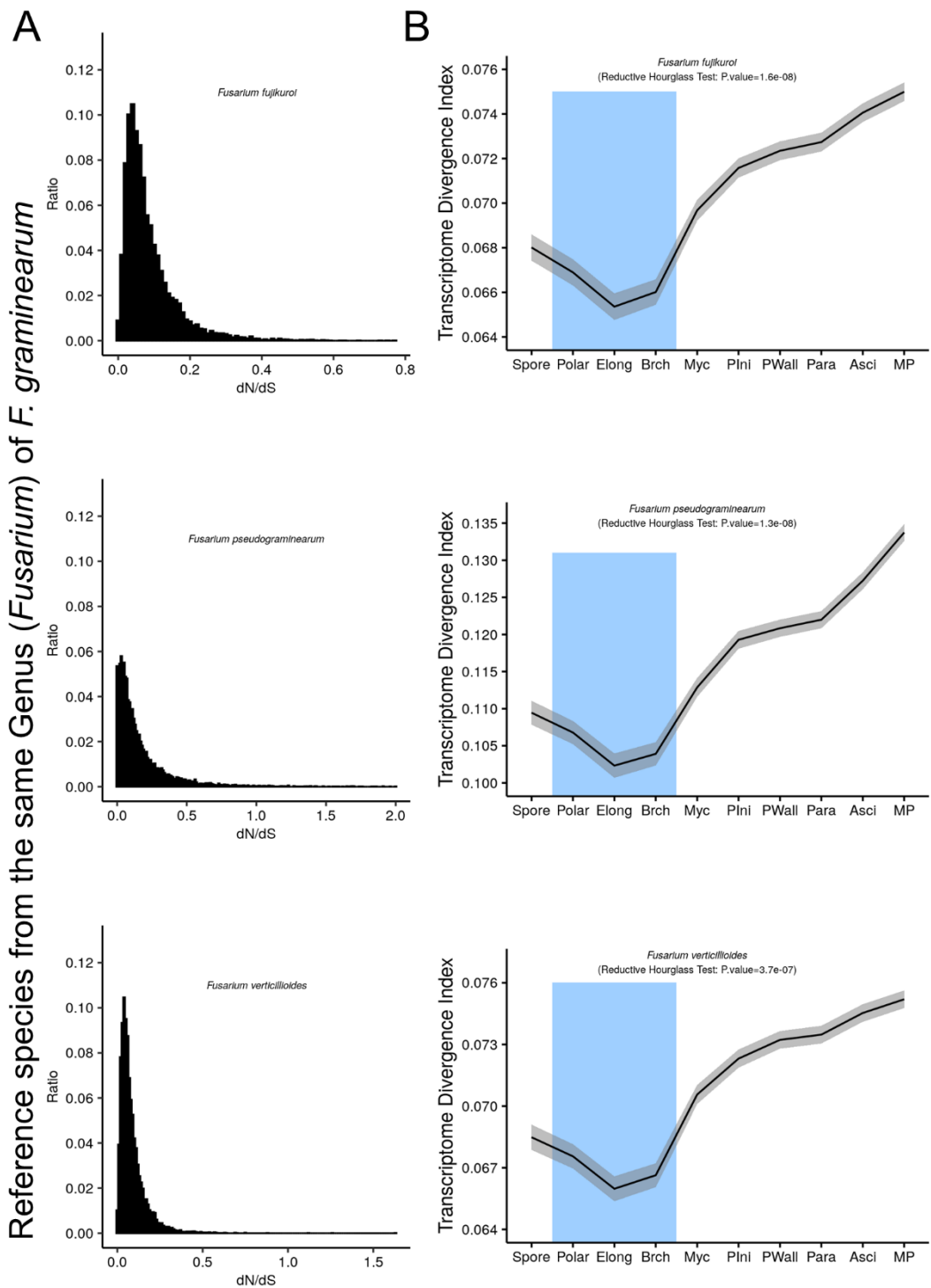


Fig. S11. Calculation of transcriptome divergence index using reference species from the same Genus (*Fusarium*) of *F. graminearum*. (A) Distribution of dN/dS ratio; (B) TDI profile, p values are derived by application of the reductive hourglass test.

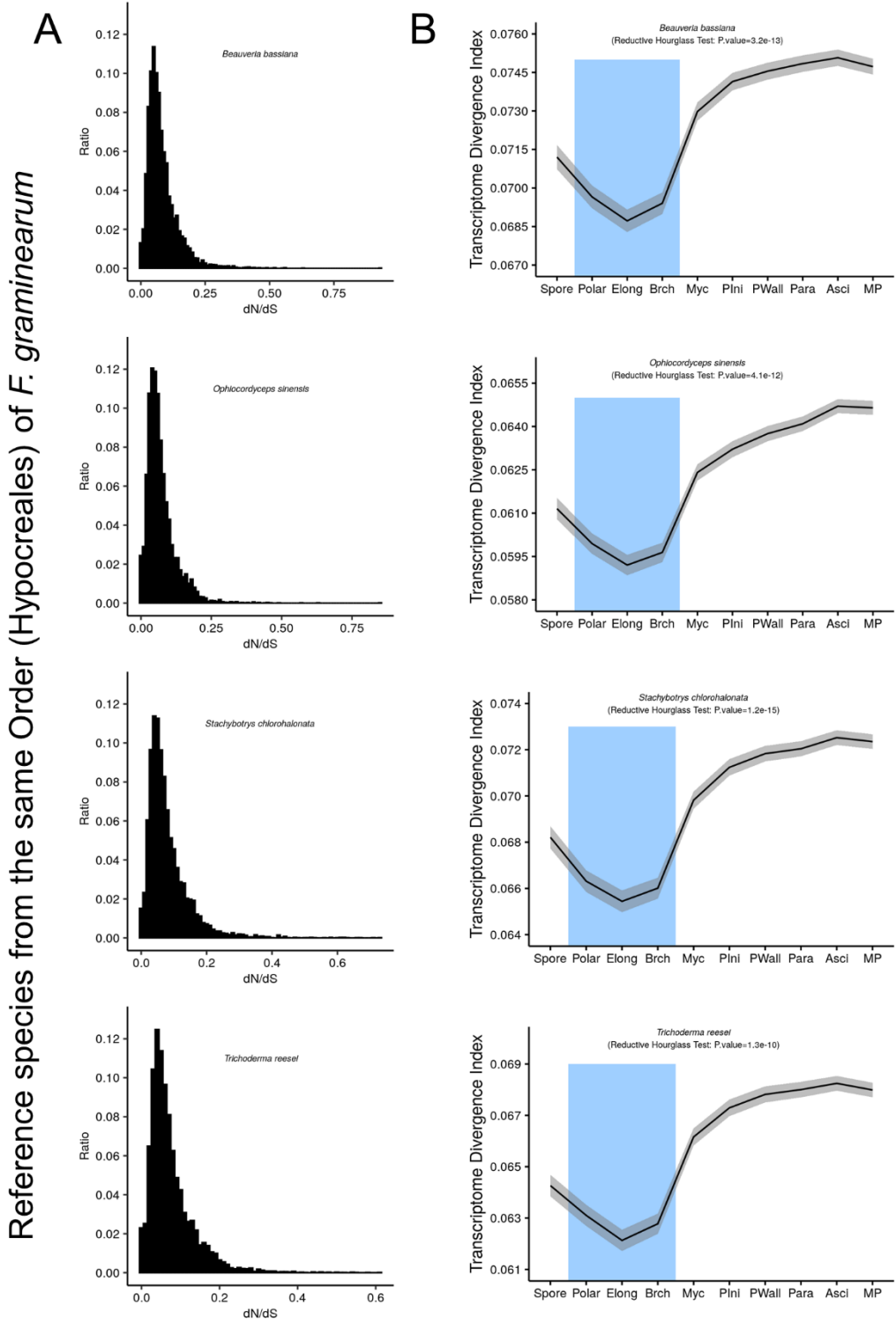


Fig. S12. Calculation of transcriptome divergence index using reference species from the same Order (Hypocreales) of *F. graminearum*. (A) Distribution of dN/dS ratio; (B) TDI profile, p values are derived by application of the reductive hourglass test.

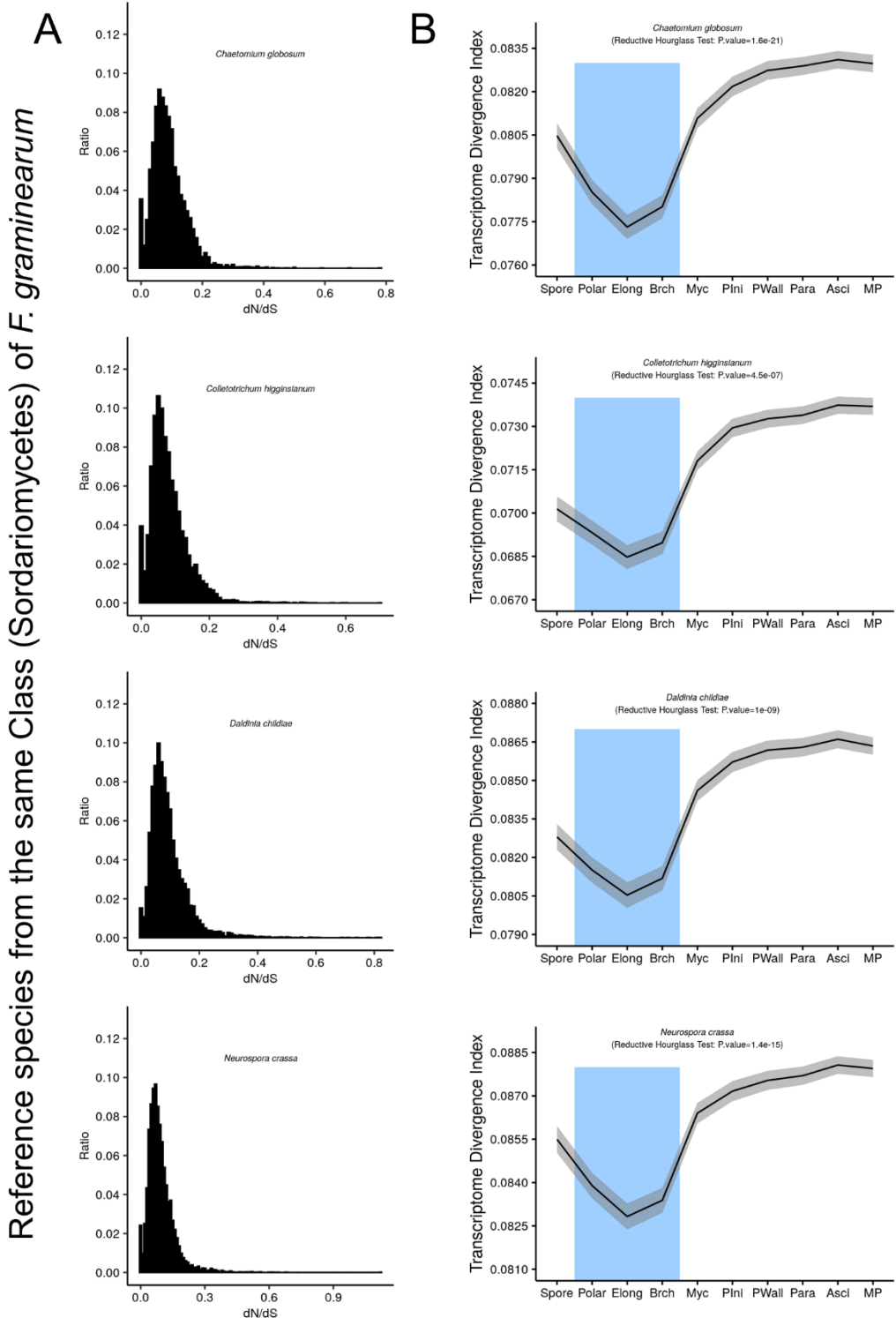


Fig. S13. Calculation of transcriptome divergence index using reference species from the same Class (Sordariomycetes) of *F. graminearum*. (A) Distribution of dN/dS ratio; (B) TDI profile, p values are derived by application of the reductive hourglass test.

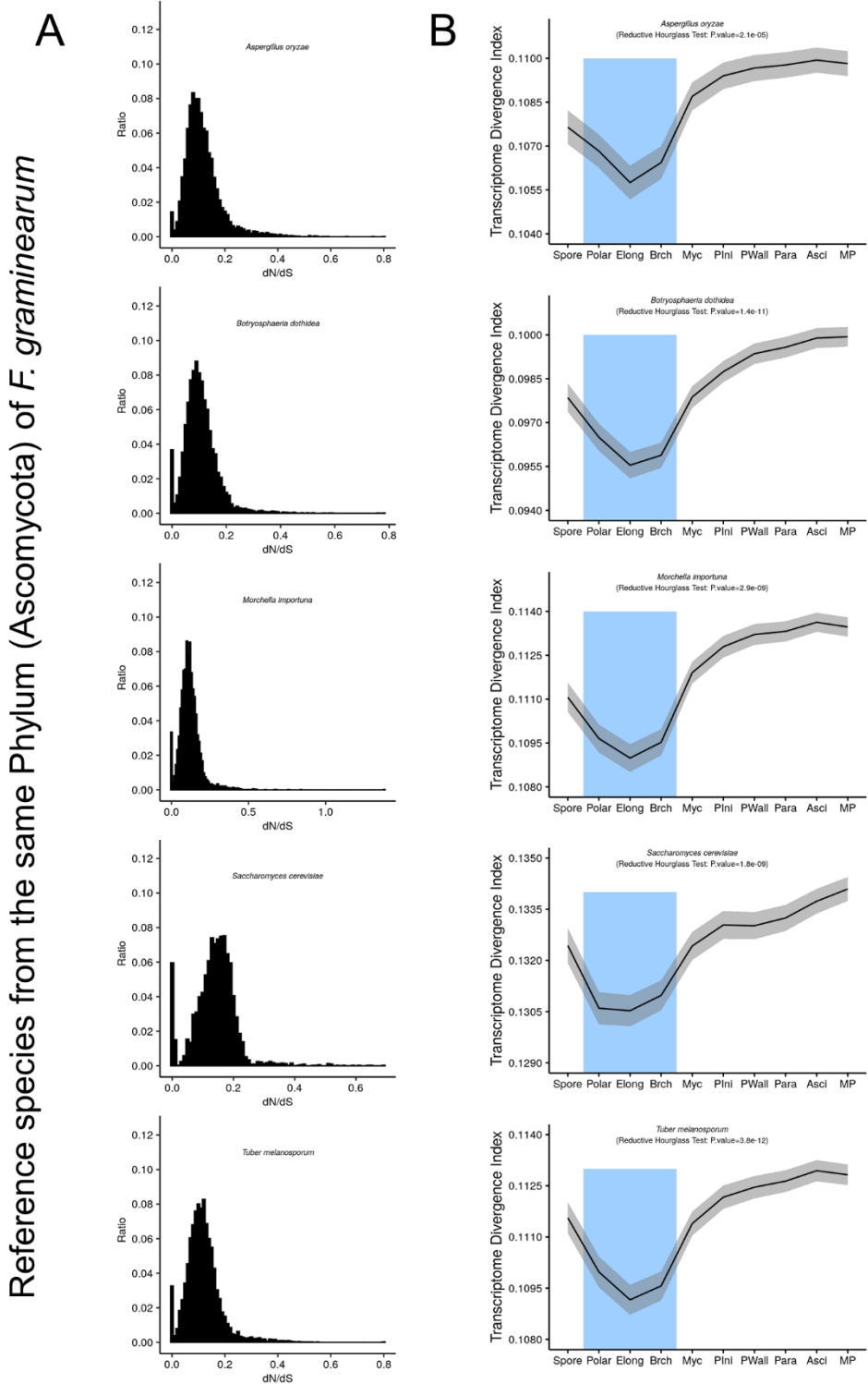


Fig. S14. Calculation of transcriptome divergence index using reference species from the same Phylum (Ascomycota) of *F. graminearum*. (A) Distribution of dN/dS ratio; (B) TDI profile, p values are derived by application of the reductive hourglass test.

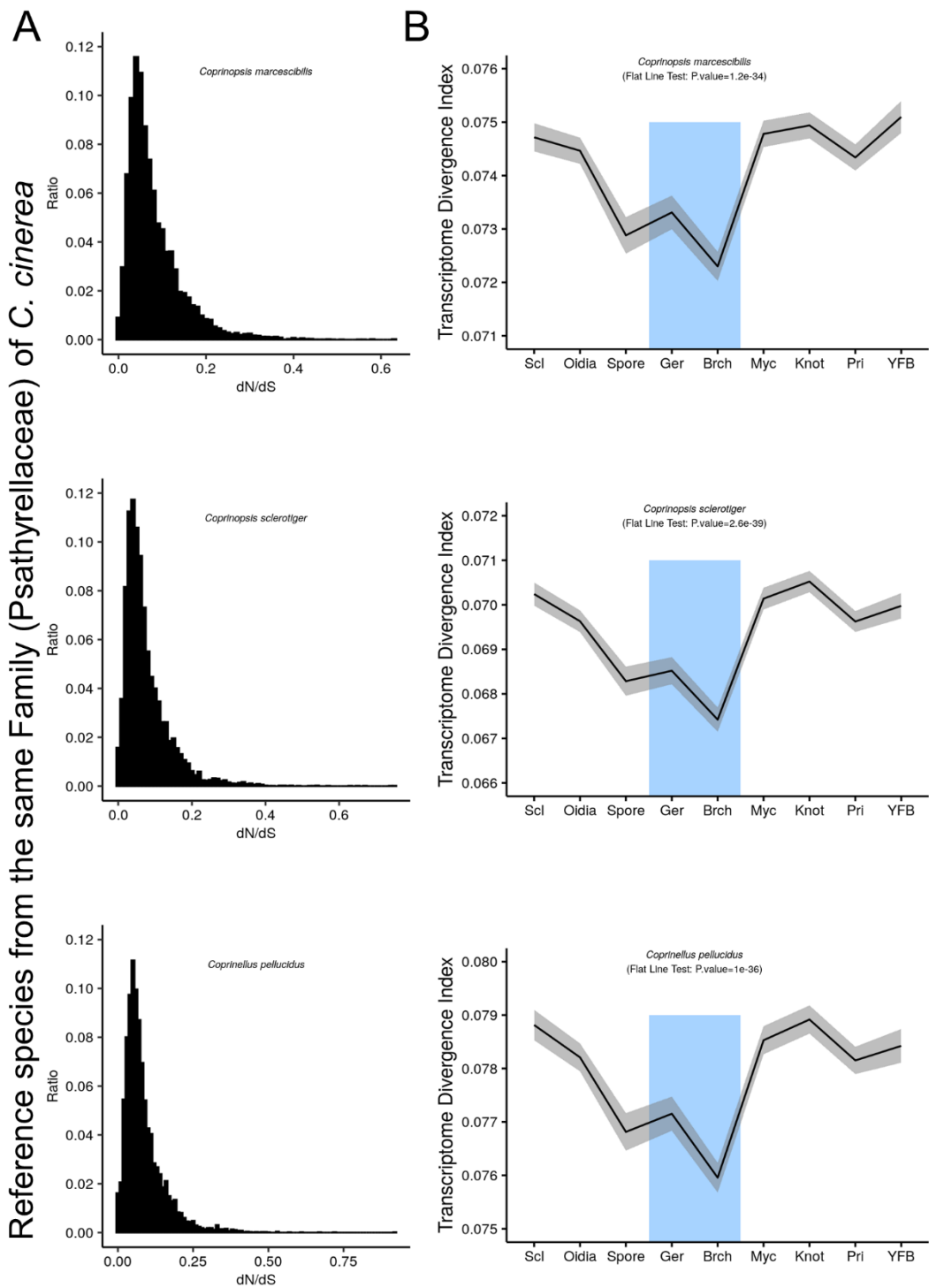


Fig. S15. Calculation of transcriptome divergence index using reference species from the same Family (Psathyrellaceae) of *C. cinerea*. (A) Distribution of dN/dS ratio; (B) TDI profile, p values are derived by application of the flat line test.

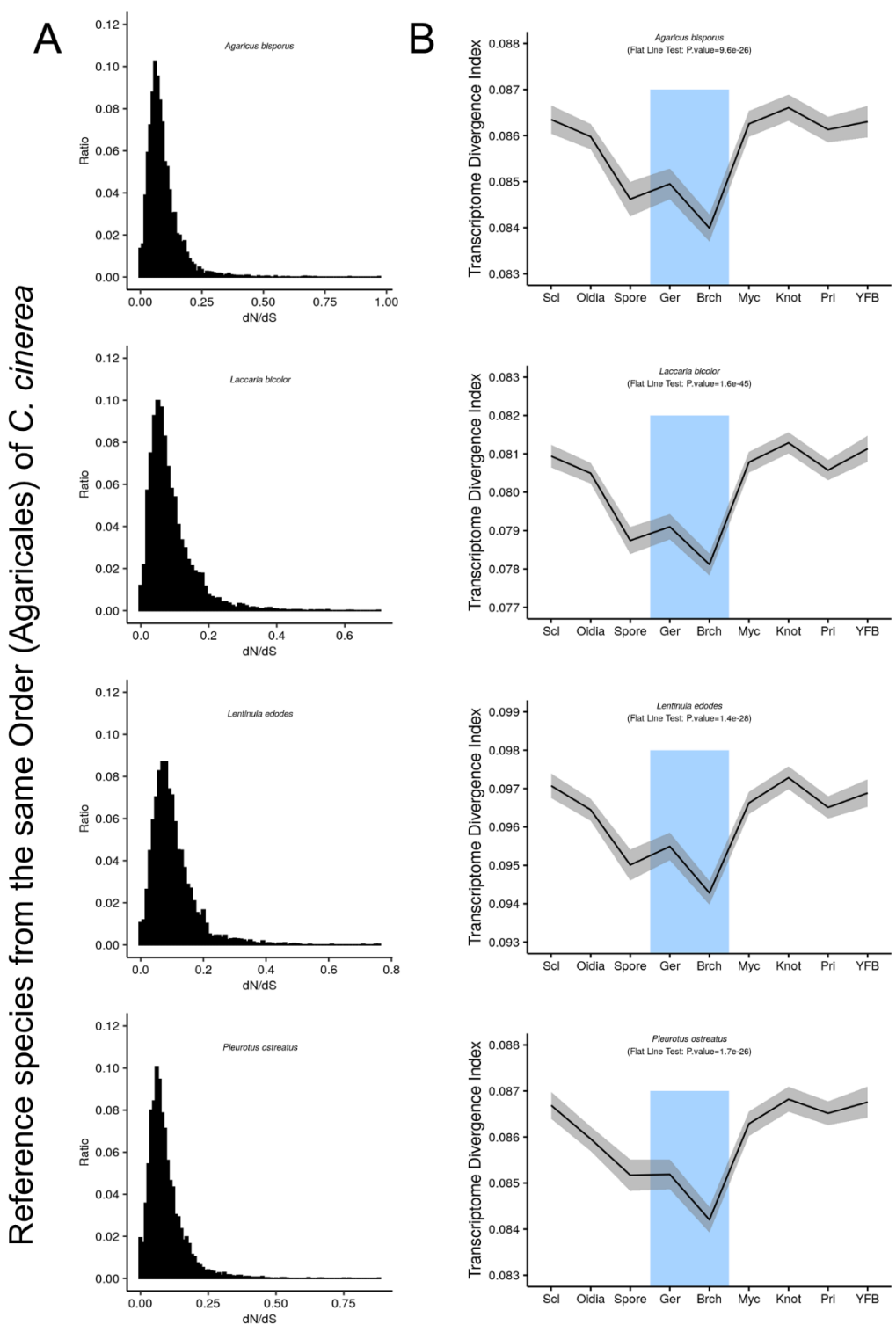


Fig. S16. Calculation of transcriptome divergence index using reference species from the same Order (Agaricales) of *C. cinerea*. (A) Distribution of dN/dS ratio; (B) TDI profile, p values are derived by application of the flat line test.

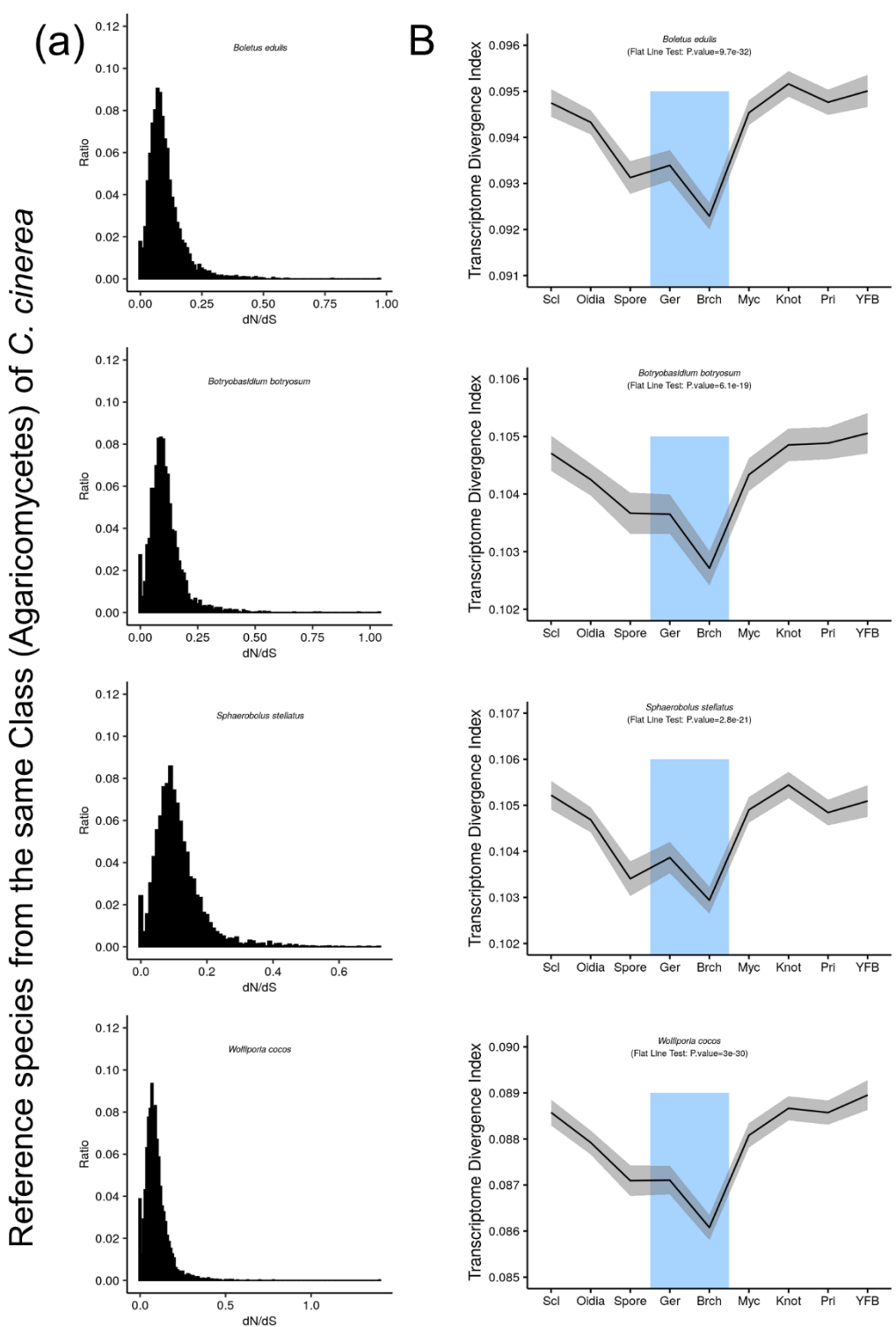


Fig. S17. Calculation of transcriptome divergence index using reference species from the same Class (Agaricomycetes) of *C. cinerea*. (A) Distribution of dN/dS ratio; (B) TDI profile, p values are derived by application of the flat line test.

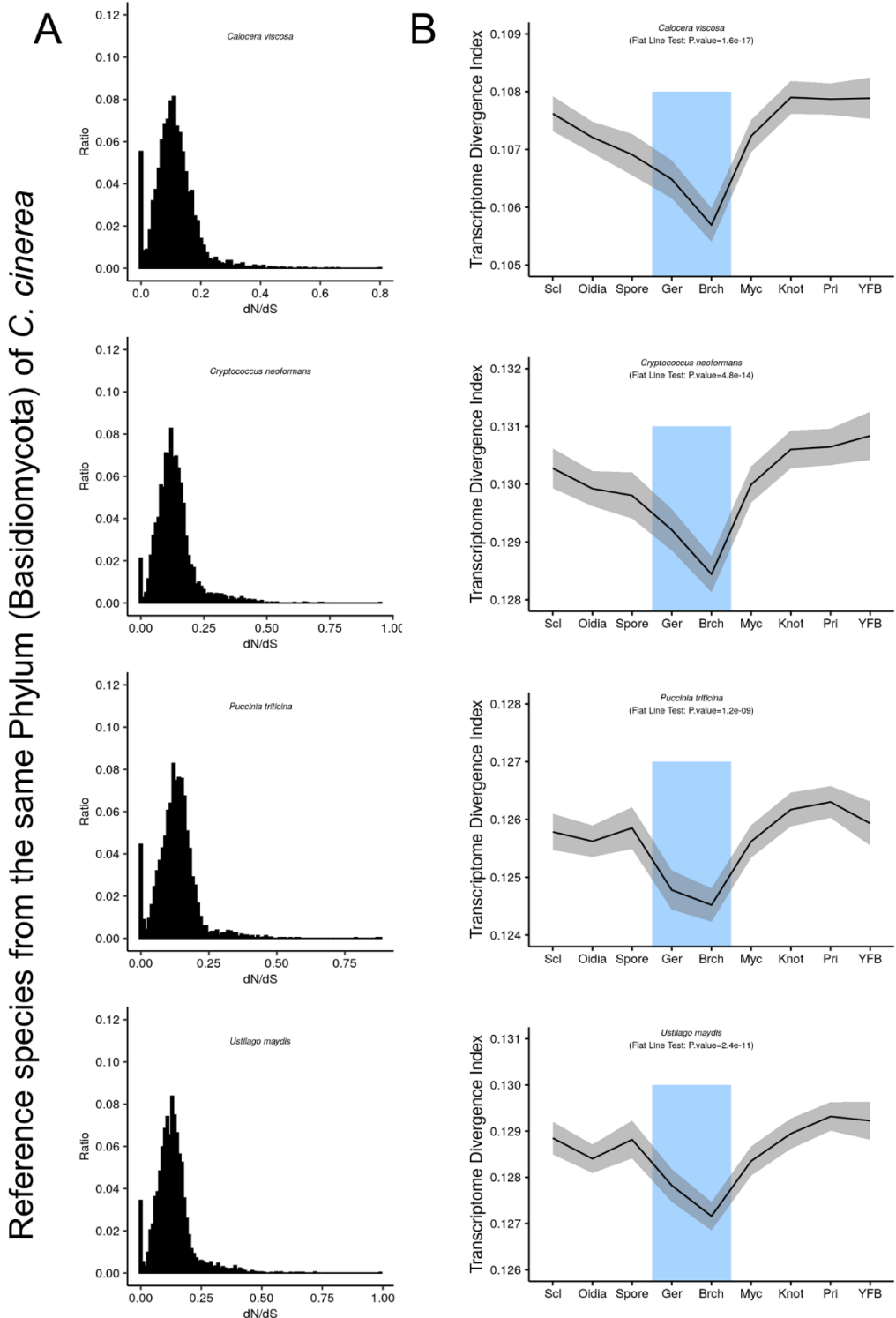


Fig. S18. Calculation of transcriptome divergence index using reference species from the same Phylum (Basidiomycota) of *C. cinerea*. (A) Distribution of dN/dS ratio; (B) TDI profile, p values are derived by application of the flat line test.

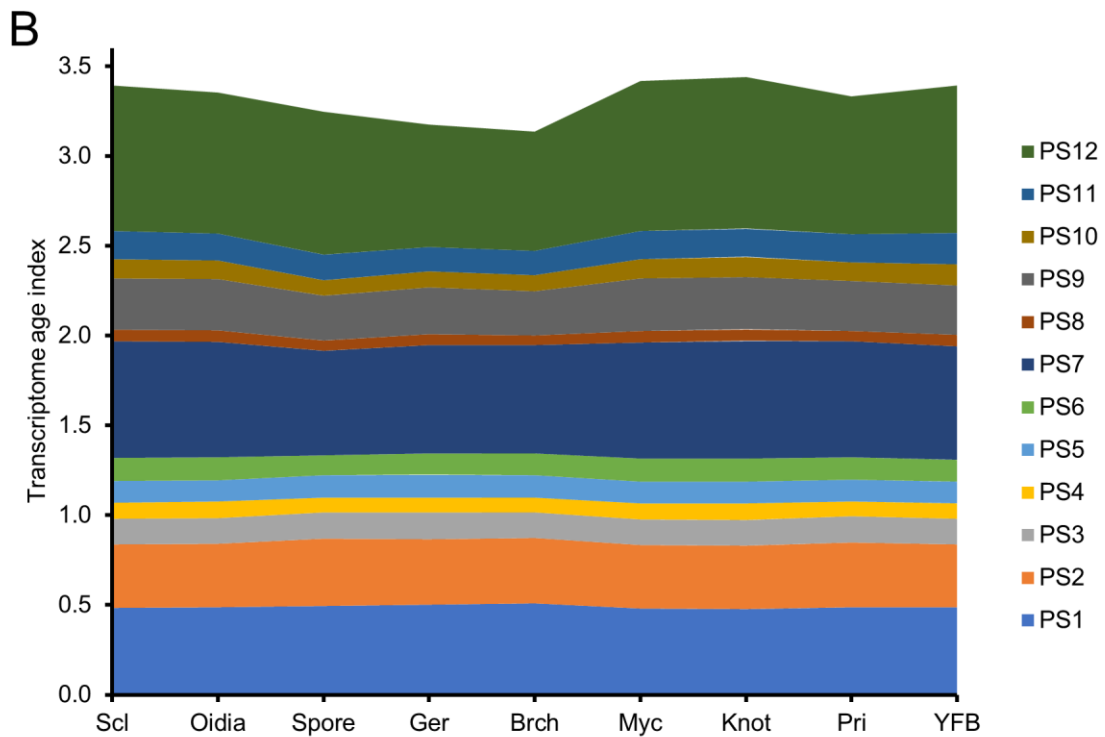
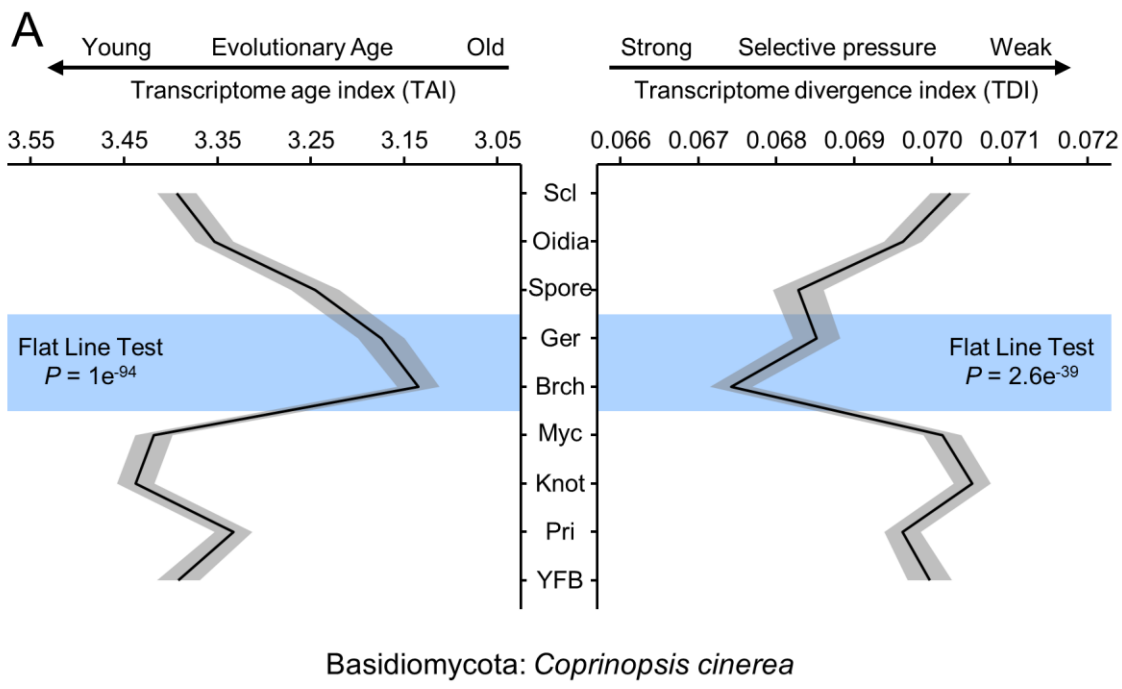


Fig. S19. Phylogenetic transcriptomic patterns of all developmental paths in *C. cinerea*. (A) TAI and TDI (*C. sclerotiger* as the reference species) profiles, p values are derived by application of the flat line test; (B) TAI split according to the genes from the different phylostrata.

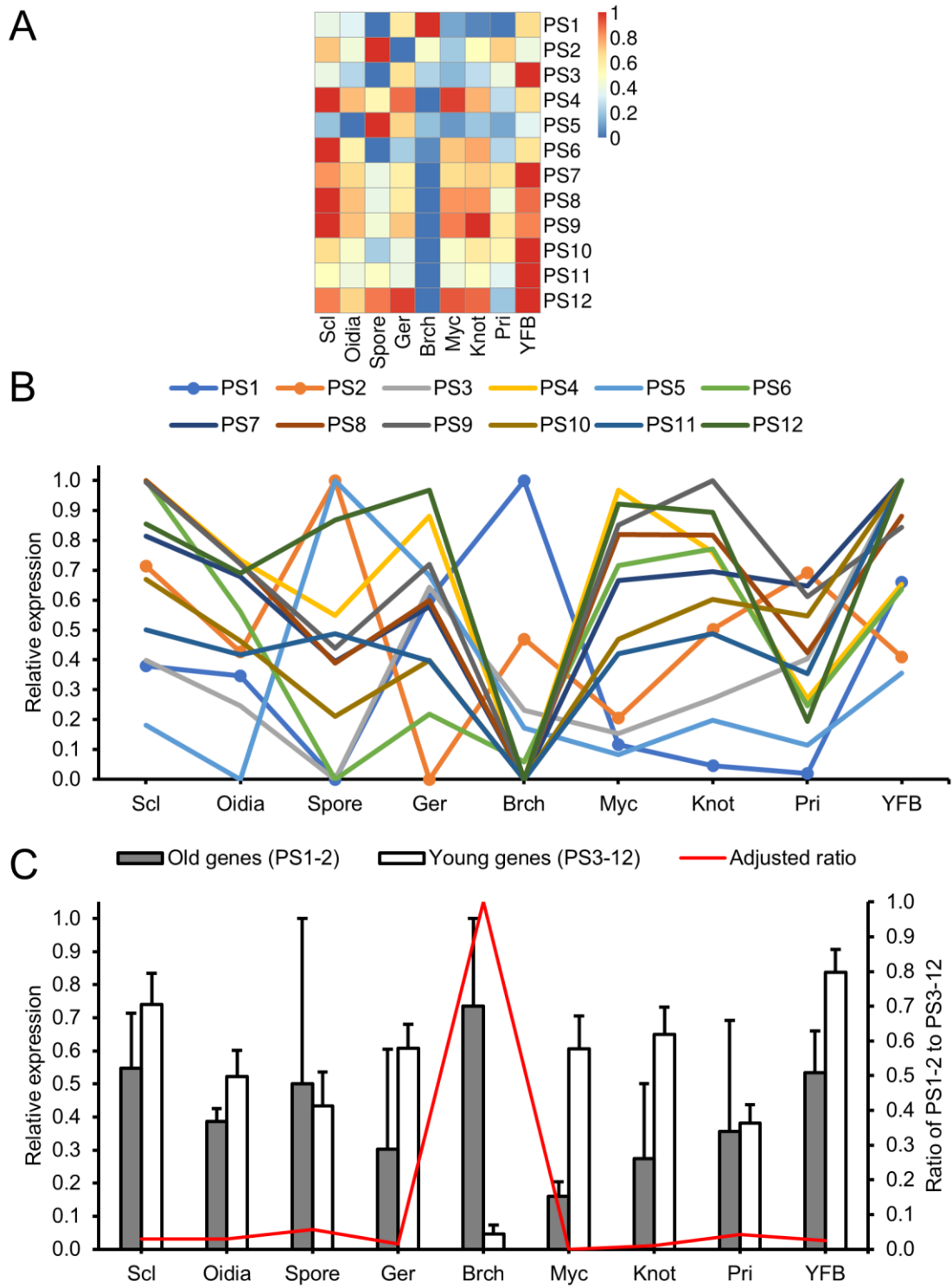


Fig. S20. Relative expression levels of genes in each phylostratum of *C. cinerea* developmental paths. (A) Heatmap on relative expression levels; (B) Line chart showing the changes on expression levels; (C) Mean relative expression levels of old genes (PS1-2) and young genes (PS3-12). Left axis is scaled for relative expression levels that showed in bars and error bars indicated standard errors, right axis is scaled for adjusted ratio of mean relative expression levels between old genes and young genes.